Inorg. Chem. **2007**, *46*, 1215−1221

Structures and Physical Properties of New Semiconducting Gold and Copper Polytellurides: $Ba_7Au_2Te_{14}$ and $Ba_{6.76}Cu_{2.42}Te_{14}$

Yanjie Cui, Abdeljalil Assoud, Jianxiao Xu, and Holger Kleinke*

Department of Chemistry, University of Waterloo, Waterloo, Ontario, Canada N2L 3G1

Received August 27, 2006

The title compounds were prepared from the elements between 600 and 800 °C in evacuated silica tubes. Both tellurides, $Ba_7Au_2Te_{14}$ and $Ba_{6.76}Cu_{2.42}Te_{14}$, form ternary variants of the $NaBa_6Cu_3Te_{14}$ type, space group $P6_3/mcm$, with $a = 14.2593(7)$ Å, $c = 9.2726(8)$ Å, and $V = 1632.8(2)$ Å^3 ($Z = 2$) for $Ba_7Au_2Te_{14}$ and $a = 14.1332(4)$ Å, $c = 9.2108(6)$ Å, and $V = 1593.3(1)$ Å^3 ($Z = 2$) for $Ba_{6.76}Cu_{2.42}Te_{14}$. The Na site is filled with a Ba atom (deficient in case of the Cu telluride) and the Cu site with 66.5(3)% Au and 61.7(8)% Cu. An additional site is filled with 9.5(7)% Cu in the structure of $Ba_{6.76}Cu_{2.42}Te_{14}$. These structures are comprised of bent Te_3^{2-} units and $AuTe_4$/$CuTe_4$ tetrahedra, forming channels filled with Ba cations. The $BaTe_9$ polyhedra are connecting the channels to a three-dimensional structure. According to the formulations $(Ba^{2+})_7(Au^+)_2(Te_3^{2-})_3(Te^{2-})_5$ and $(Ba^{2+})_{6.76}(Cu^+)_{2.42}(Te_3^{2-})_3(Te^{2-})_5$, the materials are electron-precise with 16 positive charges equalizing the 16 negative charges. Correspondingly, both tellurides are semiconductors, as experimentally confirmed, with calculated band gaps of 0.7 and 1.0 eV, respectively.

Introduction

In recent years, we have explored the thermoelectric properties of hitherto unknown materials in a number of systems. Thermoelectric materials are receiving renewed attention since the last 10 years, as is evident from groundbreaking success stories, for the most part centered around antimonides and tellurides.[1−6] The thermoelectric energy conversion can utilize a temperature gradient (e.g., from waste heat) for the creation of electricity or, vice versa, can use electricity to create a temperature gradient (mostly for cooling applications).[7,8] Typical thermoelectrics are semiconductors comprised of heavy elements[8,9] with small band gaps. These are on the order of 6 to 10 k_BT, with k_B = Boltzmann constant, T = operating temperature (i.e., 0.16−0.26 eV at room temperature).[10]

Several binary, ternary, and quaternary copper and silver chalcogenides were examined, including $Cu_{2-\delta}Te$,[11] α- and β-Ag_2Te,[12] $BaCu_2Te_2$,[13] $Ba_3Cu_{14}Te_{12}$,[14] $A_2BaCu_8Te_{10}$ (A = K, Rb, Cs),[15] $BaCu_2SnSe_4$, $BaAg_2SnSe_4$, $Ba_3Cu_2Sn_3Se_{10}$,[16] Ag_8GeTe_6,[17] AgTlTe,[18] $AgSbTe_2$,[19] $Ag_{3-\delta}Sb_{1+\delta}Te_4$,[20]

* To whom correspondence should be addressed. E-mail: kleinke@uwaterloo.ca.

(1) Sales, B. C.; Mandrus, D.; Williams, R. K. *Science* **1996**, *272*, 1325−1328.
(2) Chung, D.-Y.; Hogan, T.; Brazis, P.; Rocci-Lane, M.; Kannewurf, C.; Bastea, M.; Uher, C.; Kanatzidis, M. G. *Science* **2000**, *287*, 1024−1027.
(3) Venkatasubramanian, R.; Slivola, E.; Colpitts, T.; O'Quinn, B. *Nature* **2001**, *413*, 597−602.
(4) Hsu, K. F.; Loo, S.; Guo, F.; Chen, W.; Dyck, J. S.; Uher, C.; Hogan, T.; Polychroniadis, E. K.; Kanatzidis, M. G. *Science* **2004**, *303*, 818−821.
(5) Chung, D.-Y.; Hogan, T. P.; Rocci-Lane, M.; Brazis, P.; Ireland, J. R.; Kannewurf, C. R.; Bastea, M.; Uher, C.; Kanatzidis, M. G. *J. Am. Chem. Soc.* **2004**, *126*, 6414−6428.
(6) Brown, S. R.; Kauzlarich, S. M.; Gascoin, F.; Snyder, G. J. *Chem. Mater.* **2006**, *18*, 1873−1877.
(7) Tritt, T. M. *Science* **1999**, *283*, 804−805.
(8) DiSalvo, F. J. *Science* **1999**, *285*, 703−706.
(9) Rowe, D. M. *CRC Handbook of Thermoelectrics*; CRC Press: Boca Raton, FL, 1995.
(10) Sofo, J. O.; Mahan, G. D. *Phys. Rev. B* **1994**, *49*, 4565−4570.
(11) Sridhar, K.; Chattopadhyay, K. *J. Alloys Compd.* **1998**, *264*, 293−298.
(12) Fujikane, M.; Kurosaki, K.; Muta, H.; Yamanaka, S. *J. Alloys Compd.* **2005**, *393*, 299−301.
(13) Wang, Y. C.; DiSalvo, F. J. *J. Solid State Chem.* **2001**, *156*, 44−50.
(14) Assoud, A.; Thomas, S.; Sutherland, B.; Zhang, H.; Tritt, T. M.; Kleinke, H. *Chem. Mater.* **2006**, *18*, 3866−3872.
(15) Patschke, R.; Zhang, X.; Singh, D.; Schindler, J.; Kannewurf, C. R.; Lowhorn, N.; Tritt, T.; Nolas, G. S.; Kanatzidis, M. G. *Chem. Mater.* **2001**, *13*, 613−621.
(16) Assoud, A.; Soheilnia, N.; Kleinke, H. *Chem. Mater.* **2005**, *17*, 2255−2261.
(17) Fujikane, M.; Kurosaki, K.; Muta, H.; Yamanaka, S. *J. Alloys Compd.* **2005**, *396*, 280−282.
(18) Kurosaki, K.; Uneda, H.; Muta, H.; Yamanaka, S. *J. Alloys Compd.* **2005**, *395*, 304−306.
(19) Hagiwara, E.; Matsushita, H.; Katsui, A. *J. Adv. Sci.* **2000**, *12*, 40−41.
(20) Matsushita, H.; Hagiwara, E.; Katsui, A. *J. Mater. Sci.* **2004**, *39*, 6299−6301.

10.1021/ic061616d CCC: $37.00
Published on Web 01/23/2007

$(AgBiTe_2)_{1-\delta}(Ag_2Te)_\delta$,[21] $(AgSbTe_2)_{1-\delta}(GeTe)_\delta$,[22,23] and $AgPb_mSbTe_{2+m}$,[4] to name a few recent studies. Gold chalcogenides are appealing, as they should have similar electrical transport properties but lower thermal conductivity because of their higher molar masses. Only a few gold tellurides are known; for example, only one binary gold telluride exists, the calaverite $Au^{III}Te_2$,[24] which forms an incommensurate supercell.[25] The ternaries $CuAuSe_2$[26] and Ag_3AuTe_2[25] are also narrow gap semiconductors with trivalent gold, Au^{III}, but Cu^I and Ag^I. Here, we report on our first ternary gold telluride, which is isostructural with a (new) copper telluride, while the known binary gold and copper tellurides are quite different.

Experimental Section

Syntheses and Analyses. All reactions were commenced from the elements. These were obtained in purities of at least 99% (barium granules, 99%, from Aldrich; gold powder, spherical, −200 mesh, 99.9%, Alfa Aesar; copper powder, −625 mesh, 99.9%, Alfa Aesar; and tellurium powder, −200 mesh, 99.9%, Alfa Aesar) and were stored in an argon-filled glove box. $Ba_7Au_2Te_{14}$ was obtained in an attempt to prepare the hypothetical "$BaAuTe_2$" after starting from 1 mmol Ba, 1 mmol Au, and 2 mmol Te. This mixture was loaded into a fused silica tube within the glove box, which was then closed with a vacuum valve and transferred to a vacuum line. There, the tube was sealed under dynamic vacuum of approximately 10^{-2} mbar. The tube was heated to 800 °C within 48 h employing a resistance furnace, kept at that temperature for 2 h, and then cooled to 200 °C with a ramp of 3 °C per hour; this was followed by switching off the furnace. This reaction yielded at least one unknown material, besides unreacted gold, as was evident from the X-ray powder diagram (INEL) obtained from the ground sample. After solving this structure via single-crystal structure determination, described later, all peaks of the powder diagram could be assigned to this new material, namely, $Ba_7Au_2Te_{14}$, and elemental gold.

Subsequently, phase-pure $Ba_7Au_2Te_{14}$ was synthesized via the same method, including the same temperature profile, starting from the stoichiometric 7:2:14 ratio. Attempts to synthesize analogous copper and silver tellurides were successful only in the case of copper, and no isostructural selenide was found. The copper analogue was prepared using the same temperature profile, but a subsequent single-crystal structure study revealed a significant deviation from the 7:2:14 ratio of the elements, which was observed for $Ba_7Au_2Te_{14}$, namely, $Ba_{6.76}Cu_{2.42}Te_{14}$. Attempts to prepare phase-pure stoichiometric $Ba_7Cu_2Te_{14}$ failed, but a reaction starting from the elements in the refined ratio of 6.76:2.42:14 yielded a pure sample without noticeable side products (analyzed via powder diffraction).

Energy-dispersive X-ray analysis (EDAX), using the electron microscope LEO 1530 with an additional EDAX device, EDAX Pegasus 1200, did not reveal any heteroelements, such as silicon that might have come from the silica tube. The distribution of the elements Ba, Cu/Au, and Te was homogeneous throughout the sample. Averaged over five crystals, the Ba/Au/Te ratio was 29.5:8.4:62.0 in atomic %, which compares well with the refined 7:2:14 ratio (≡30.4:8.7:60.9). For the Cu sample, we calculated the Ba/Cu/Te ratio to 28.6:9.0:62.3 in atomic %, which is in reasonable agreement with the refined ratio of 6.76:2.42:14 (≡29.2:10.4:60.4).

Crystal Structure Determinations. The Smart Apex CCD (Bruker), equipped with an area detector utilizing graphite-monochromated Mo Kα radiation, was employed for the data collection. In each case, 606 frames were measured with exposure times of 60 s each. The data were corrected for Lorentz and polarization effects. Absorption corrections were based on fitting a function to the empirical transmission surface, as sampled by multiple equivalent measurements of numerous reflections.[27]

The unit cell dimensions indicated the adoption of the $NaBa_6Cu_3Te_{14}$ type, hexagonal space group $P6_3/mcm$.[28] Therefore, the refinements using the SHELXTL package[29] commenced from that structure model, with Ba on the Na site (Ba2). In the case of the gold compound, Au was assumed to sit on the Cu position. That refinement converged to residual factors of R1 = 0.0794 and wR2 = 0.2130 (observed data). Because of the conspicuously high displacement factor of the Au site (0.0415(6) Å^2), its occupancy was refined, resulting in 66.5(3)%, an inconspicuous displacement factor of 0.0241(2) Å^2, and lower R values, namely, R1 = 0.0369 and wR2 = 0.0702. On the other hand, while the displacement factor of Ba2 was significantly higher than that of Ba1, refining the occupancy of Ba2 revealed full occupancy within one standard deviation, without a change in the residual values.

In the case of the copper compound, the refinements yielded clear deficiencies of both sites in question, with refined occupancies of 61.7(8)% for Cu1 and 76(1)% for Ba2. This led to lowered R values; for example, R1 decreased from 0.0550 to 0.0428. The difference Fourier map comprised an additional peak of 6 e/Å^3, surrounded by three Te atoms at distances of 2.5 and 2 × 2.8 Å. This position was subsequently refined as a deficient Cu site, Cu2, with an occupancy of 9.5(7)%, a procedure that further decreased R1 to 0.0369.

In the end, the refined formulas of the two compounds were $Ba_7Au_{1.995(9)}Te_{14}$ and $Ba_{6.76(1)}Cu_{2.42(7)}Te_{14}$. Crystallographic details are given in Table 1, and atomic positions, displacement, and occupancy factors are given in Table 2.

Electronic Structure Calculations. The electronic structures were calculated using the self-consistent tight-binding first principles LMTO method (LMTO = linear muffin tin orbitals) with the atomic spheres approximation (ASA).[30,31] In the LMTO approach, the density functional theory is employed utilizing the local density approximation (LDA) for the exchange correlation energy.[32] The following wave functions were used: for Ba 6s, 5d, 4f, and 6p included via the downfolding technique;[33] for Au 6s, 6p, 5d, and 5f (downfolded); for Cu 4s, 4p, and 3d; and for Te 5s, 5p, and 5d and 4f (the latter two downfolded). The 252 independent *k* points

(21) Sakakibara, T.; Imoto, T.; Takigawa, Y.; Kurosawa, K. *J. Adv. Sci.* **2001**, *12*, 392−396.
(22) Skrabek, E. A.; Trimmer, D. S. In *CRC Handbook of Thermoelectrics*; Rowe, D. M., Ed.; CRC Press: Boca Raton, FL, 1995; pp 267−275.
(23) Shelimova, L. E.; Konstantinov, P. P.; Karpinsky, O. G.; Avilov, E. S.; Kretova, M. A.; Fleurial, J. P. *Intern. Conf. Thermoelectr.* **1999**, *18*, 536−540.
(24) Wang, J.; Lu, X.-g.; Sundman, B.; Su, X. *J. Alloys Compd.* **2006**, *407*, 106−111.
(25) Young, D. P.; Brown, C. L.; Khalifah, P.; Cava, R. J.; Ramirez, A. P. *J. Appl. Phys.* **2000**, *88*, 5221−5224.
(26) Park, Y.; Kanatzidis, M. G. *Inorg. Chem.* **2001**, *40*, 5913−5916.
(27) *SAINT*, version 4; Siemens Analytical X-ray Instruments Inc.: Madison, WI, 1995.
(28) Zhang, X.; Schindler, J. L.; Hogan, T.; Albritton-Thomas, J.; Kannewurf, C. R.; Kanatzidis, M. G. *Angew. Chem., Int. Ed. Engl.* **1995**, *34*, 68−71.
(29) Sheldrick, G. M. *SHELXTL*, version 5.12; Siemens Analytical X-Ray Systems: Madison, WI, 1995.
(30) Andersen, O. K. *Phys. Rev. B* **1975**, *12*, 3060−3083.
(31) Skriver, H. L. *The LMTO Method*; Springer: Berlin, Germany, 1984.
(32) Hedin, L.; Lundqvist, B. I. *J. Phys. C: Solid State Phys.* **1971**, *4*, 2064−2083.
(33) Lambrecht, W. R. L.; Andersen, O. K. *Phys. Rev. B* **1986**, *34*, 2439−2449.

Table 1. Crystallographic Data of $Ba_7Au_2Te_{14}$ and $Ba_{6.76}Cu_{2.42}Te_{14}$

refined formula	$Ba_7Au_{1.995(9)}Te_{14}$	$Ba_{6.76(1)}Cu_{2.42(7)}Te_{14}$
formula weight [g/mol]	3141.71	2868.59
T of measurement [K]	298(2)	298(2)
wavelength [Å]	0.71073	0.71073
crystal system	hexagonal	hexagonal
space group	$P6_3/mcm$	$P6_3/mcm$
a [Å]	14.2593(7)	14.1332(4)
c [Å]	9.2726(8)	9.2108(6)
V [Å^3]	1632.8(2)	1593.3(1)
Z	2	2
ρ_{calcd} [g/cm^3]	6.390	5.979
R1 and wR2 (all data)[a]	0.0403, 0.0715	0.0378, 0.0803
R1 and wR2 ($I > 2\sigma(I)$)[a]	0.0369, 0.0702	0.0369, 0.0799
min; max electron density [e$^-$/Å^3]	−2.02 at 0.578, 0.457, 1/4 [1.63 Å from Te3]; +2.26 at 0.818, 0.300, 1/4 [0.72 Å from Ba1]	−3.11 at 0, 0.150, 1/4 [0.36 Å from Te1]; +3.30 at 0, 0.296, 0.018 [0.59 Å from Te2]

[a] $R1 = \sum||F_o| - |F_c||/\sum|F_o|$; $wR2 = [\sum[w(F_o^2 - F_c^2)^2]/\sum[w(F_o^2)^2]]^{1/2}$.

Table 2. Atomic Coordinates and Equivalent Displacement Parameters of $Ba_7Au_2Te_{14}$ (top) and $Ba_{6.76}Cu_{2.42}Te_{14}$ (bottom)

atom	site	x	y	z	U_{eq}[a]/Å^2	occ.
Ba1	12j	0.45267(3)	0.21083(3)	1/4	0.01216(10)	1
Ba2	2b	0	0	1/2	0.0348(3)	1
Te1	6g	0.18356(5)	0	1/4	0.02083(17)	1
Te2	12k	0.33229(4)	0.33229(4)	0.02535(6)	0.01525(12)	1
Te3	6g	0.47277(5)	0.47277(5)	1/4	0.01393(14)	1
Te4	4d	2/3	1/3	0	0.01241(15)	1
Au1	6g	0.19410(5)	0.19410(5)	1/4	0.0241(2)	0.665(3)
Ba1	12j	0.45096(4)	0.20789(4)	1/4	0.0146(1)	1
Ba2	2b	0	0	1/2	0.066(1)	0.76(1)
Te1	6g	0.17585(6)	0	1/4	0.0354(3)	1
Te2	12k	0.32582(4)	0.32582(4)	0.02718(6)	0.0216(1)	1
Te3	6g	0.46933(5)	0.46933(5)	1/4	0.0175(2)	1
Te4	4d	2/3	1/3	0	0.0143(2)	1
Cu1	6g	0.1952(2)	0.1952(2)	1/4	0.0232(7)	0.617(8)
Cu2	12k	0.155(1)	0.155(1)	0.089(2)	0.042(5)	0.095(7)

[a] U_{eq} is defined as one-third of the trace of the orthogonalized U_{ij} tensor.

of the first Brillouin zone were chosen via an improved tetrahedron method.[34] To model the electron-precise formula $Ba_7M_2Te_{14}$, all Ba sites were treated as fully occupied, the Cu2 site was ignored, and four of the six Au/Cu1 sites per unit cell were filled, resulting in the right formula and a symmetry reduction reflected in the orthorhombic space group *Cmcm*. The molecular orbital diagram of the V-shaped Te_3^{2-} unit of $Ba_7Au_2Te_{14}$, point group C_{2v}, was calculated using Gaussian[35] via the B3LYP method with the 3-21G basis set.[36]

Transport Measurements. The phase-pure samples were pressed into bar-shaped pellets of the dimensions 6 × 1 × 1 [in mm] for physical transport measurements since no single crystals of sufficient dimensions were available. Silver paint (Ted Pella) was used to create the electric contacts. The commercial thermopower measurement apparatus (MMR Technologies) was employed for the determination of the Seebeck coefficient, S. The S was measured under dynamic vacuum in the temperature range between 300 and 550 K, using constantan as an internal standard to determine the temperature difference. The specific electrical conductivity, σ, was determined using a four-point method; a homemade device was used to determine the voltage drops ΔV over distances (L) of approximately 2 mm at currents below 5 mA under dynamic vacuum between 320 and 160 K. The achieved densities were between 81 and 84% of the theoretical maximum, as determined via the single-crystal structure studies. The resistances (R) were calculated from the voltage drops using Ohm's law, that is, $R = \Delta V/I$, with I = current. We calculated $\sigma(T)$ after measuring the lengths between the contacts, L, according to $\sigma = L/(AR)$, with the area $A = 1$ mm × 1 mm.

Results and Discussion

Crystal Structures. The two new ternary tellurides, $Ba_7Au_{1.995(9)}Te_{14}$ and $Ba_{6.76(1)}Cu_{2.42(7)}Te_{14}$, for simplicity called $Ba_7M_2Te_{14}$, crystallize in substitution variants of the $NaBa_6Cu_3Te_{14}$ structure, briefly described in a communication,[28] where the Na site is filled with Ba2. A second Cu site, Cu2, is partly filled in the case of the ternary Cu telluride, which may be seen as a split position of Cu1. The crystal structure of $Ba_7M_2Te_{14}$ is comprised of MTe_4 tetrahedra, which are interconnected through corners to form planar M_3Te_3 rings, which in turn are connected to Te_3 units. The rings are stacked along [001], surrounding the Ba2 atoms. Nine-fold Te-coordinated Ba1 atoms connect the rings in the *a*,*b* plane, and additional Te atoms, Te4, are located between six Ba1 atoms. Figure 1 shows a projection of the $Ba_7M_2Te_{14}$ structure along the *c*-axis, highlighting the covalent M−Te and Te−Te interactions.

The Ba1−Te bonds (Table 3) are inconspicuous, ranging from 3.50 to 3.66 Å ($Ba_7Au_2Te_{14}$) and from 3.51 to 3.64 Å ($Ba_{6.76}Cu_{2.42}Te_{14}$). The nine-folded coordination of Ba1 compares well with the nine Ba−Te bonds per Ba atom in $BaSbTe_3$ (3.41−3.89 Å),[37] Ba_2SnTe_5 (3.44−3.84 Å),[38] and

(34) Blöchl, P. E.; Jepsen, O.; Andersen, O. K. *Phys. Rev. B* **1994**, *49*, 16223−16233.

(35) Frisch, M. J.; Trucks, G. W.; Schlegel, H. B.; Scuseria, G. E.; Robb, M. A.; Cheeseman, J. R.; Zakrzewski, V. G.; Montgomery, J. A., Jr.; Stratmann, R. E.; Burant, J. C.; Dapprich, S.; Millam, J. M.; Daniels, A. D.; Kudin, K. N.; Strain, M. C.; Farkas, O.; Tomasi, J.; Barone, V.; Cossi, M.; Cammi, R.; Mennucci, B.; Pomelli, C.; Adamo, C.; Clifford, S.; Ochterski, J.; Petersson, G. A.; Ayala, P. Y.; Cui, Q.; Morokuma, K.; Malick, D. K.; Rabuck, A. D.; Raghavachari, K.; Foresman, J. B.; Cioslowski, J.; Ortiz, J. V.; Stefanov, B. B.; Liu, G.; Liashenko, A.; Piskorz, P.; Komaromi, I.; Gomperts, R.; Martin, R. L.; Fox, D. J.; Keith, T.; Al-Laham, M. A.; Peng, C. Y.; Nanayakkara, A.; Gonzalez, C.; Challacombe, M.; Gill, P. M. W.; Johnson, B. G.; Chen, W.; Wong, M. W.; Andres, J. L.; Head-Gordon, M.; Replogle, E. S.; Pople, J. A. *Gaussian 98*, revision A.7; Gaussian, Inc.: Pittsburgh, PA, 1998.

(36) Pietro, W. J.; Francl, M. M.; Hehre, W. J.; DeFrees, D. J.; Pople, J. A.; Binkley, J. S. *J. Am. Chem. Soc.* **1982**, *104*, 5039−5048.

(37) Volk, K.; Cordier, G.; Cook, R.; Schäfer, H. *Z. Naturforsch., B: Chem. Sci.* **1980**, *35*, 136−140.

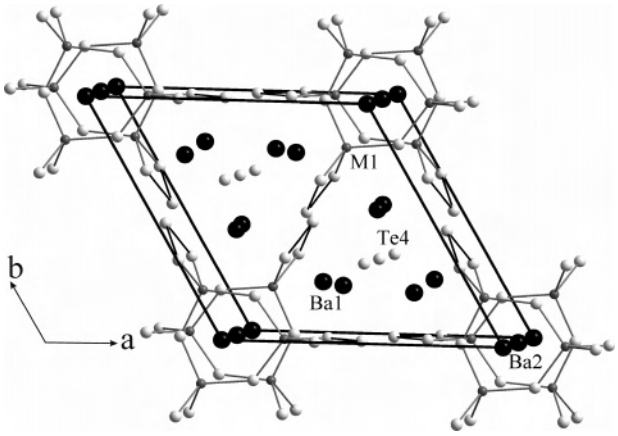

Figure 1. Crystal structure of $Ba_7M_2Te_{14}$ (excluding the M2 site). Black circles, Ba; dark gray, Cu/Au; bright gray, Te.

Table 3. Selected Interatomic Distances [Å] of $Ba_7Au_2Te_{14}$ and $Ba_{6.76}Cu_{2.42}Te_{14}$

		$Ba_7Au_2Te_{14}$	$Ba_{6.76}Cu_{2.42}Te_{14}$
Ba1−Te1		3.4967(7)	3.5110(7)
Ba1−Te2	2×	3.6412(5)	3.6147(5)
Ba1−Te2	2×	3.6528(5)	3.6170(5)
Ba1−Te3		3.6004(6)	3.5723(6)
Ba1−Te3		3.6557(7)	3.6348(7)
Ba1−Te4	2×	3.5222(4)	3.5121(3)
Ba2−Te1	6×	3.4964(6)	3.3881(7)
M1−Te1	2×	2.6957(5)	2.6329(15)
M1−Te2	2×	2.8674(7)	2.7602(18)
M2−Te1	2×		2.778(11)
M2−Te1			3.14(2)
M2−Te2			2.483(16)
Te2−Te3	2×	2.8900(7)	2.8855(8)
Te1−Te2	2×	3.319(1)	3.318(1)

$Ba_3Cu_{14}Te_{12}$ (3.47−3.84 Å).[14] Similarly, the Ba2−Te bonds of the $Ba2Te_6$ octahedron (3.50 Å in $Ba_7Au_2Te_{14}$ and 3.39 Å in $Ba_{6.76}Cu_{2.42}Te_{14}$) are reminiscent of the bonds in BaTe (3.42 Å, NaCl type).[39]

In $Ba_7Au_2Te_{14}$, the four Au1−Te bonds of 2 × 2.70 Å and 2 × 2.87 Å, averaged to 2.78 Å, are longer than expected for Au^{III}, as found in the sylvanite $AgAuTe_4$ (four bonds between 2.67 and 2.69 Å),[40] and $CrAuTe_4$ (4 × 2.68 Å).[41] Moreover, the tetrahedral Cu1 coordination sphere with distances of 2.63−2.76 Å for $Ba_{6.76}Cu_{2.42}Te_{14}$ is typical for Cu^{I}; for example, the Cu^{I}−Te bonds of $BaCu_2Te_2$ range from 2.59 to 2.81 Å,[13] and in $Ba_3Cu_{14}Te_{12}$, they range from 2.50 to 2.85 Å.[14] The coordination of the Cu2 site is highly irregular, with distances to Te atoms of 2.49, 2 × 2.78, and 3.14 Å. It is noted that the shortness of the Cu1−Cu2 distance (1.59 Å) necessitates that the two positions are never filled at the same location within the crystal. This concurs well with the combined occupancies being below 100% (62% for Cu1 and 10% for Cu2). Such a scenario is common in copper chalcogenides, for example, in $LnCu_{0.3-0.4}Te_2$,[42] $CuGd_3Cu_2Te_7$,[43] $Cu_{2-\delta}Se$,[44] $CuSm_3Se_6$,[45] and in $Cu_4Bi_4Se_9$[46] but not in gold chalcogenides.

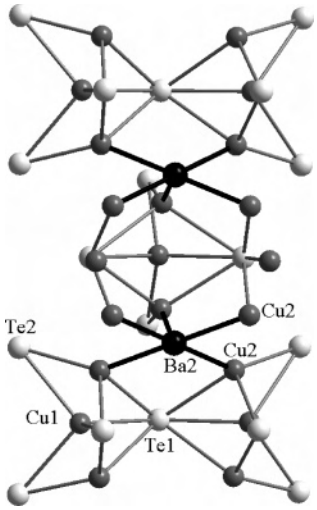

Figure 2. Three Cu_3Te_3 rings stacked along [001], showing both the Cu1 and Cu2 atoms. Black circles, Ba; dark gray, Cu; bright gray, Te.

The shortness of the Cu2−Ba2 distance of 2.33 Å requires that these two positions are not occupied at the same location either. Because of the low occupancies of 10% for Cu2 and 76% for Ba2, this can be realized in the whole crystal. As a consequence of this scenario, the Cu atoms cannot migrate from one ring to the other along the *c*-axis, as the Ba2 site, where filled, would prevent this (Figure 2). Since the rings are well-separated in the *a*,*b* plane, any Cu ion movement is restricted to occur only locally within a Cu_3Te_3 ring.

Figure 3 compares the planar $Cu1_3Te_3$ and puckered $Cu2_3Te_3$ rings, including the attached V-shaped Te_3 units. These rings are staggered along the *c*-axis (6_3 screw axis running through their center), thereby surrounding the Ba2 cation with six Te atoms in octahedral coordination.

The presence of the Cu2 site seems to have an impact onto the Te1 site, which is part of the Cu_3Te_3 ring, as the Te1 site exhibits strong anisotropies in the displacement factors, reflected in a U_{33}/U_{11} ratio of 4.8:1, with $U_{11} \approx U_{22}$. The corresponding Te1 of $Ba_7Au_2Te_{14}$ exhibits a smaller, more regular U_{33}/U_{11} ratio of 2.7:1, also with $U_{11} \approx U_{22}$. Similar U_{33}/U_{11} ratios were observed for the Au1 and Cu1 sites, indicating a tendency to deviate from the planarity of the M_3Te_3 ring. It is noted that none of these sites could be refined as a split site. Moreover, lowering the symmetry to allow for nonplanarity by selecting the space group $P6_3cm$ did not lead to any improvements or a significant nonplanarity of this ring.

The Te_3 units, formed by the Te2 and Te3 atoms, exhibit rather small Te−Te−Te angles, 92.2° in the gold and 90.7° in the copper telluride. Its Te−Te bonds are somewhat longer than single bonds (2.89 Å each in both cases). Treating this

(38) Assoud, A.; Derakhshan, S.; Soheilnia, N.; Kleinke, H. *Chem. Mater.* **2004**, *16*, 4193−4198.
(39) Spangenberg, K. *Naturwissenschaften* **1927**, *15*, 266−266.
(40) Pertlik, F. *Tschermaks Mineral. Petrogr. Mitt.* **1984**, *33*, 203−212.
(41) Reynolds, T. K.; McGuire, M. A.; DiSalvo, F. J. *J. Solid State Chem.* **2004**, *177*, 2998−3006.
(42) Huang, F. Q.; Brazis, P.; Kannewurf, C. R.; Ibers, J. A. *J. Am. Chem. Soc.* **2000**, *122*, 80−86.
(43) Huang, F. Q.; Ibers, J. A. *J. Solid State Chem.* **2001**, *159*, 186−190.
(44) Machado, K. D.; de Lima, J. C.; Grandi, T. A.; Campos, C. E. M.; Maurmann, C. E.; Gasperin, A. A. M.; Souza, S. M.; Pimenta, A. F. *Acta Crystallogr., Sect. B* **2004**, *60*, 282−286.
(45) Strobel, S.; Schleid, T. *J. Solid State Chem.* **2003**, *171*, 424−428.
(46) Makovicky, E.; Sotofte, I.; Karup-Moller, S. *Z. Kristallogr.* **2002**, *217*, 597−604.

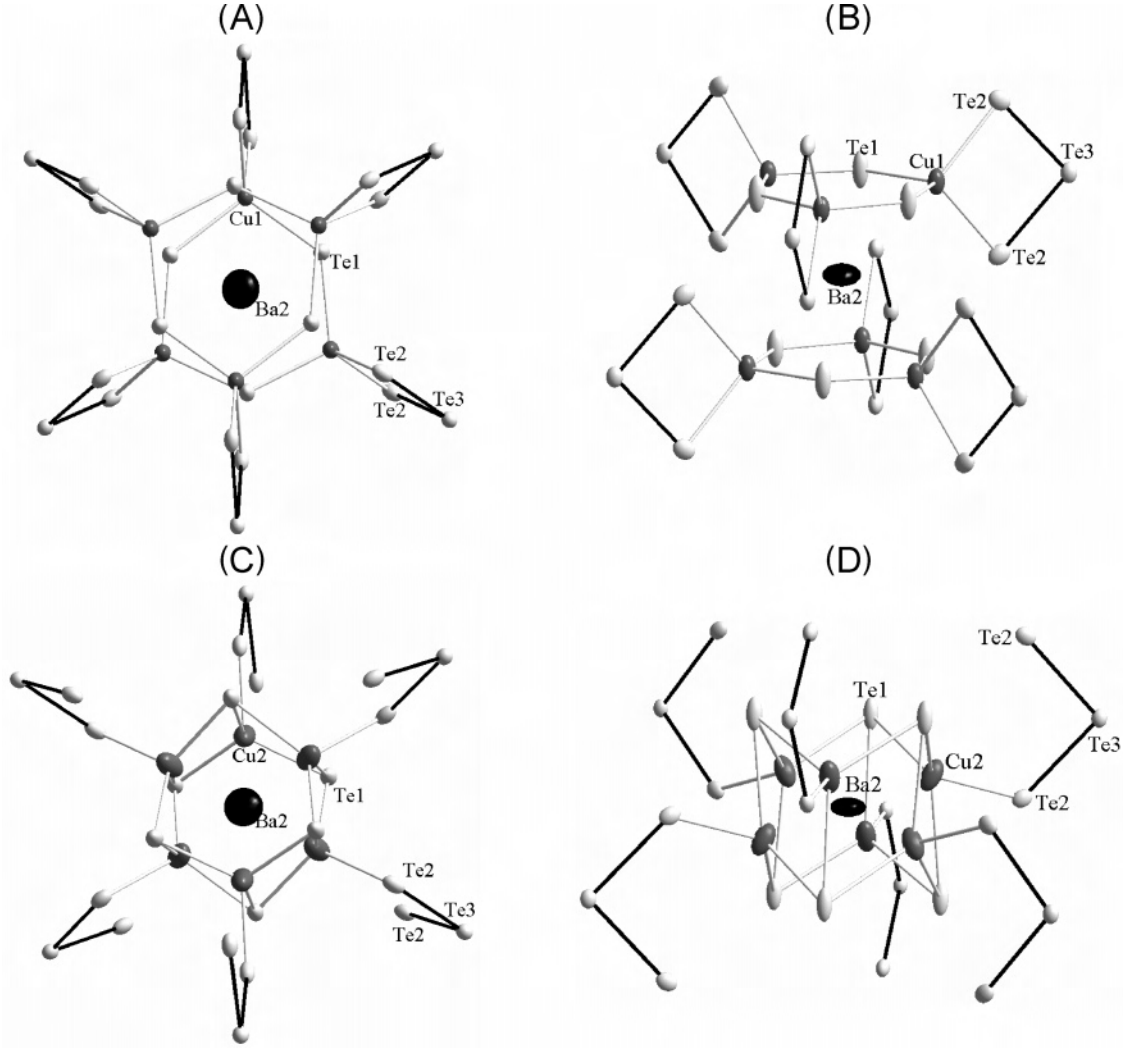

Figure 3. Top: Two $Cu1_3Te_3$ rings, including the attached Te_3 units surrounding the Ba2 atom (ellipsoid presentation). Black circles, Ba; dark gray, Cu; bright gray, Te. (A) Viewed along the *c*-axis; (B) projected onto the *a*,*c* plane. Bottom: Two $Cu2_3Te_3$ rings, including the attached Te_3 units surrounding the Ba2 atom. (C) Viewed along the *c*-axis; (D) projected onto the *a*,*c* plane.

unit as a classical Te_3^{2-} unit and the Te1 and Te4 atoms as Te^{2-}, one obtains 16 negative charges for the 14 Te atoms per formula unit. However, there is an additional Te−Te contact (Te1−Te2) of 3.32 Å between the Cu_3Te_3 rings, which stands against a full octet on Te1. A partial electron transfer from the $Te1^{2-}$ to the Te_3^{2-} group might be the cause for the elongated Te2−Te3, resulting in a $Te1^{(2-x)-}$ and a $Te_3^{(2+x)-}$ unit,[47] which ultimately does not change the overall electron balance and allows for the Te1−Te2 contact.

The valency of Cu in $Na^I(Ba^{II})_6(Cu^I)_3Te_{14}$ was identified as +I, giving 16 positive (and 16 negative) charges per formula unit. Assuming the same for Au in $Ba_7Au_2Te_{14}$, that is, Au^I, in accord with the Au−Te distances, one obtains 16 positive charges as well. Again postulating Cu^I, the positive charges of $Ba_{6.76}Cu_{2.42}Te_{14}$ sum up to $6.76 \times 2 + 2.42 = 15.94$. This formalism supports the refined occupancies, yielding 2.42 Cu atoms per formula unit, hence the existence of Cu2, since both ternary tellurides exhibit 16 positive charges per formula unit, like $Na^I(Ba^{II})_6(Cu^I)_3Te_{14}$. Similarly, the K analogue was reported with K/Ba mixed occupancies combined with Cu deficiencies (but no Cu2 site) and a refined formula of $(K_{0.60}Ba_{0.40})_6Cu_{2.58}Te_{14}$, that is, 15.98 positive charges.[28]

Electronic Structures. The calculated densities of states (DOS) of the models, $Ba_7M_2Te_{14}$, are depicted in Figure 4. In both cases, a forbidden gap separates the valence band from the conduction band, with the Au telluride exhibiting the smaller gap ($E_{gap} = 0.7$ versus 1.0 eV). Again in both cases, the top of the valence band and the bottom of the conduction band are dominated by Te p states. The Au d states dominate the area below −4 eV at the bottom of the valence band, while the Cu d states mostly occur between −2 and −4 eV.

To gain insight into the character of the two different Te−Te contacts, the crystal orbital Hamilton population curves[48,49] of both interactions in both structure models are compared

(47) Papoian, G. A.; Hoffmann, R. *Angew. Chem., Int. Ed.* **2000**, *39*, 2408−2448.

(48) Dronskowski, R.; Blöchl, P. E. *J. Phys. Chem.* **1993**, *97*, 8617−8624.
(49) Glassey, W. V.; Hoffmann, R. *J. Chem. Phys.* **2000**, *113*, 1698−1704.

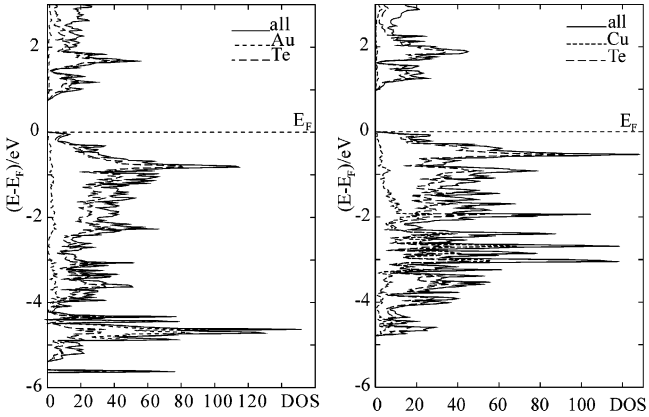

Figure 4. Densities of states of $Ba_7Au_2Te_{14}$ (left) and $Ba_7Cu_2Te_{14}$ (right). The Fermi level, E_F, was arbitrarily placed at 0 eV.

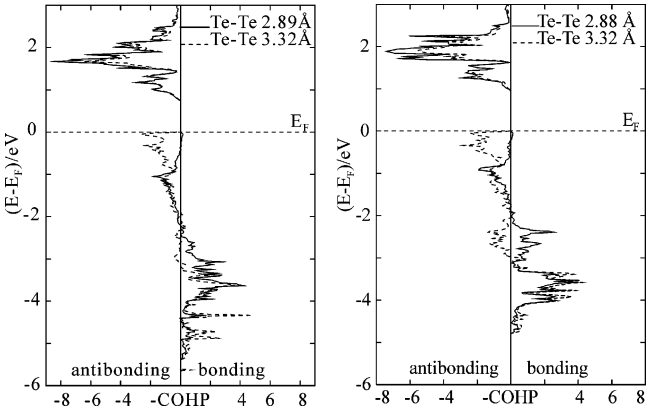

Figure 5. Selected crystal orbital Hamilton population curves of $Ba_7Au_2Te_{14}$ (left) and $Ba_7Cu_2Te_{14}$ (right). The Fermi level, E_F, was arbitrarily placed at 0 eV.

in Figure 5. The curves of the two tellurides are quite similar. It is evident that the shorter bond within each compound, that is, the one within the Te_3^{2-} group, is much stronger; the longer ones exhibit filled antibonding states above −1 eV, where the short ones are nonbonding. Moreover, the former are anti- to nonbonding between −3.2 and −2 eV, and the latter are bonding. The rest of the curves are comparable. The integration up to the Fermi level reveals that all four of the shown interactions have net bonding character, reflected in negative integrated COHP values (ICOHPs).[50] For the Au compound, these are −1.54 eV (2.89 Å) and −0.17 eV (3.32 Å), and for the Cu compound, they are −1.61 eV (2.88 Å) and −0.12 eV (3.32 Å). Thus, the shorter bonds appear to be stronger by factors of 9 and 13, respectively.

The molecular orbital diagram of an isolated Te_3^{2-} unit is shown in Figure 6, again with the s orbitals situated below the chosen energy window. The energies are given in hartree, $E_h = 2$ Ry $= 27.2$ eV. Therein, the bonding and antibonding π molecular orbitals are filled, yielding an only σ-bonded ion. Two σ bonds are present, reflected in the filled molecular orbitals of a_1 and b_2 symmetry. Therefore, it is justified to treat this ion as a classical σ-bonded Te_3^{2-} unit. A large gap separates the HOMO from the LUMO, which is also present

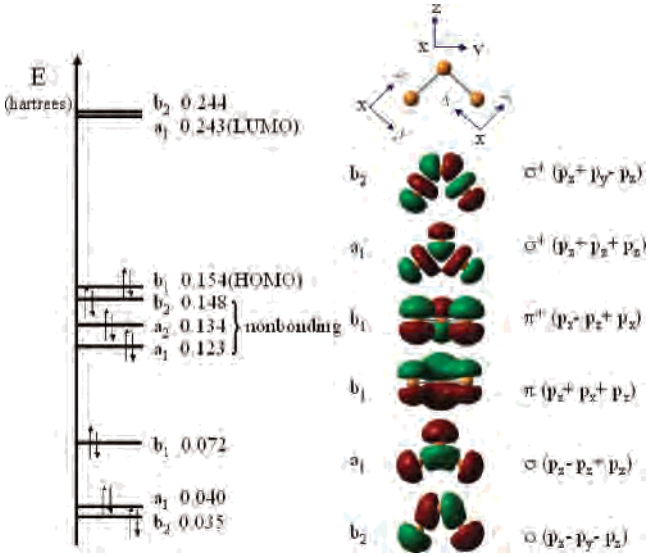

Figure 6. MO diagram of the V-shaped Te_3^{2-} unit.

in the COHP curve of this Te−Te interaction in the three-dimensional crystal structure.

Physical Properties. The electronic structure calculations predicted semiconducting behavior. This was confirmed by our experiments; the exponential increase of the electrical conductivity with increasing temperature, as observed for both tellurides (left part of Figure 7), is typical for semiconductors. The electrical conductivity is higher in the case of $Ba_7Au_2Te_{14}$, with a room-temperature value of 1.6 $m\Omega^{-1}$ cm^{-1}, compared to 70 $\mu\Omega^{-1}$ cm^{-1} for $Ba_{6.76}Cu_{2.42}Te_{14}$. Because of the strong temperature dependence combined with the low conductivity at room temperature, the current and hence the conductivity of the Cu sample could not be determined below 255 K. The lower values of $Ba_{6.76}Cu_{2.42}Te_{14}$ were expected based on the smaller band gap of the Au material. For comparison, the room-temperature values of $Na^{I}(Ba^{II})_6(Cu^{I})_3Te_{14}$ and $(K_{0.60}Ba_{0.40})_6Cu_{2.58}Te_{14}$ were reported to be 100 and 10 $(\mu\Omega)^{-1}$ cm^{-1}, respectively, measured on single crystals. Advanced thermoelectrics typically exhibit an electrical conductivity above 1000 Ω^{-1} cm^{-1}.[4]

For intrinsic semiconductors, Arrhenius's Law for thermally activated conduction applies: $\ln\sigma/\sigma_0 = \exp(-\Delta_A/k_BT)$, with Δ_A = activation energy = 1/2 E_{gap}.[51] Then, plotting $\ln\sigma$ versus $1/T$ results in a linear curve with a slope of $-1/2\ E_{gap}/k_B$. In the case of the Cu sample, we obtained such a linear curve over the whole temperature range, that is, above 255 K, with a regression coefficient of $R^2 = 0.9999$ and $E_{gap} = 0.6$ eV. In the case of the Au sample, where the conductivity was measured down to 160 K, a significant deviation from the linearity was noticed, expressed in the low $R^2 = 0.982$. This is likely a consequence of extrinsic charge carriers that cause a smaller slope at low temperatures.[52] Linearity was observed above 255 K, comparable to

(50) Landrum, G. A.; Dronskowski, R. *Angew. Chem., Int. Ed.* **2000**, *39*, 1560−1585.

(51) Kittel, C. *Introduction to Solid State Physics*, 7th ed.; John Wiley & Sons, Inc.: New York, 1996.

(52) Greig, D. *Electrons in Metals and Semiconductors*; McGraw-Hill: London, U.K., 1969.

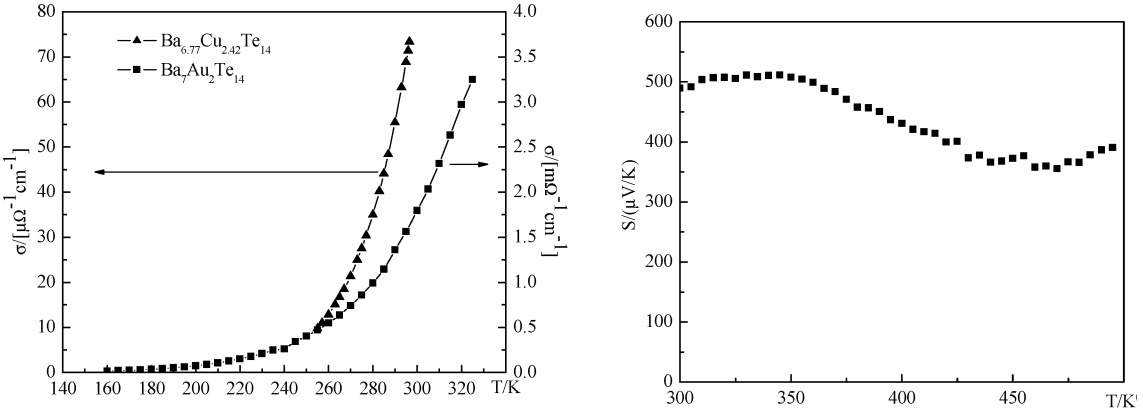

Figure 7. Electrical conductivity (left) of $Ba_7Au_2Te_{14}$ and $Ba_{6.76}Cu_{2.42}Te_{14}$ and Seebeck coefficient measurements of $Ba_7Au_2Te_{14}$ (right).

the slope of the Cu conductivity, with $R^2 = 0.9989$ and $E_{gap} = 0.4$ eV, which is evidently smaller than the 0.6 eV of the Cu compound. These results qualitatively confirm the trend of the gaps as calculated with the LMTO approach, that is, the gap is smaller in the case of the Au compound (calculated to be 0.7 eV, compared to 1.0 eV for the Cu compound).

Because of the small electrical conductivity of $Ba_{6.76}Cu_{2.42}Te_{14}$, its Seebeck coefficient could not be determined. The Seebeck coefficient for $Ba_7Au_2Te_{14}$ at 300 K is around $+490$ μV/K and decreases to $+355$ μV/K at 470 K (right part of Figure 7). The charge carriers of $Na^{I}(Ba^{II})_6(Cu^{I})_3Te_{14}$ were predominantly p type as well, with a Seebeck coefficient of $+100$ μV/K.

Conclusions

Two new tellurides, $Ba_7Au_2Te_{14}$ and $Ba_{6.76}Cu_{2.42}Te_{14}$, were synthesized and structurally characterized. Both are variants of the $NaBa_6Cu_3Te_{14}$ type, where an additional site is occupied by Cu2 in the case of $Ba_{6.76}Cu_{2.42}Te_{14}$. The Cu delocalization is restricted to occur within the Cu_3Te_3 rings only, that is, no Cu ion conductivity may be observed. Since the monovalent Na cation is replaced by the divalent Ba cation, the Au/Cu position exhibits deficiencies in both ternary compounds, with occupancies of 66.5(3)% Au and 61.7(8)% Cu on Cu1 and 9.5(7)% Cu on Cu2. In accordance with the Cu content being higher than the Au content, there are deficiencies on one Ba site (Ba2) in the case of the ternary copper compound, which are also required because of the short Ba2−Cu2 distance. Assuming that Na, Cu, and Au are in the +I state, there are 16 positive charges in all cases, within the standard deviations ($Ba_7Au_{1.995(9)}Te_{14}$: 15.995(9); $Ba_{6.76(1)}Cu_{2.42(7)}Te_{14}$: 15.9(1)), equalizing the 16 negative charges of the 14 Te sites, considered as five Te^{2-} and three Te_3^{2-} units.

Both materials are semiconductors, with calculated gaps of 0.7 and 1.0 eV. These gaps are larger than ideal for the thermoelectric energy conversion, which is reflected in a low electrical conductivity of both materials.

Acknowledgment. Financial support from NSERC, CFI, OIT (Ontario Distinguished Researcher Award for H.K.), the Province of Ontario (Premier's Research Excellence Award for H.K.), and the Canada Research Chair program (CRC for H.K.) is appreciated.

Supporting Information Available: Two X-ray crystallographic files (CIF), two experimental powder diagrams, and two lnσ, 1/T diagrams. This material is available free of charge via the Internet at http://pubs.acs.org.

IC061616D